

A Compilation Scheme for Suppressing Crosstalk and Decoherence in Superconducting Quantum Chips with Tunable Coupling and Tunable Qubits

Bin-Han LU (University of Science and Technology of China)

Yu-Chun Wu (Key Laboratory of Quantum Information, Chinese Academy of Sciences,
School of Physics, University of Science and Technology of China)

Guo-Ping Guo (University of Science and Technology of China)

Peng Wang (University of Science and Technology of China)

Abstract—Crosstalk is a major source of noise in quantum computing. When quantum gates are executed in parallel, the interaction frequencies of the qubits will be resonant, resulting in unwanted residual coupling, which reduces the fidelity of the quantum gates. Current crosstalk solutions are difficult to eliminate crosstalk globally on the chip. In this paper, we propose an Optimizing Qubit Mapping and Gate Scheduling Scheme for Crosstalk Mitigation and Decoherence Suppression. We first extend a pulse compensation crosstalk cutoff scheme from adiabatic gate system to tunable coupler and tunable qubit system. We then present a two-step compilation framework. The first step is to select the qubit mapping scheme according to the crosstalk and decoherence noise, and the second step is to optimize the gate timing using the maximum-independent set problem in graph theory. Evaluation shows that for tunable qubits and tunable couplers architecture, pulse compensation reduces the quantum gates error caused by crosstalk by up to two orders of magnitude. Compared with the compilation scheme without considering crosstalk, our scheme can significantly mitigate crosstalk and improve the fidelity of algorithm execution. Compared with the existing crosstalk-aware compilation schemes, our scheme can more effectively reduce the decoherence noise while suppressing crosstalk. Moreover, our algorithm complexity is polynomial with the circuit size.

I. INTRODUCTION

Quantum computing has entered the era of noisy intermediate-scale quantum (NISQ) chips. NISQ superconducting quantum chips consist of dozens to hundreds of qubits, which are not large enough to support fault-tolerant quantum computing and are susceptible to noise [24], [26], [27]. Therefore, finding schemes to suppress noise is critical [1].

In this article, we mainly focus on quantum computing techniques based on superconducting transmon qubits. Superconducting quantum chips have two sources of dominant noise. (1) Decoherence noise refers to the process of losing the coherence of quantum states in a quantum system due to the interaction with the environment [6], [15], [38]. Decoherence error will accumulate as quantum program execution time increases. (2) Crosstalk noise, due to the unwanted qubit coupling between concurrent qubit operations under near-resonant frequency, the error of parallel execution of multiple quantum gates will be significantly higher than that of isolated execution. [20]. Crosstalk can lead to a five to ten-fold increase

in error for two-qubit gates executed in parallel [4], [39]. To address the first problem, shortening the execution time of quantum programs to ensure that quantum computation is completed before the qubit states fully decohere is necessary. Solutions in [3], [31], [32] optimize qubit mapping to reduce the execution time after compilation. The optimized mapping algorithm for decoherence noise above aims to reduce the execution time of the algorithm by making the two-qubit gates execute in parallel, but due to the existence of crosstalk, parallelism will dramatically increase the gate error. If quantum gates have to be executed serially to mitigate crosstalk, the time optimization benefits of the optimized mapping scheme will be greatly diminished.

Crosstalk is the unwanted coupling between qubits when two qubits have frequencies near resonant. To reduce crosstalk noise, the hardware-based solutions includes i) qubit architecture design [11], [21], adding compensation microwave to the resonant qubits, ii) frequency allocation which tune qubit frequencies apart from collision [29], [35]. These schemes mitigate the crosstalk of qubits during the execution of single-qubit gates. However in tunable qubits architecture such as Google’s system [12], when executing two-qubit gates, the frequencies of the qubits and the coupler will change to the interaction frequencies, which increases the effective coupling between the gate qubits and the neighboring qubits. This will invalidate the crosstalk cutoff between the neighboring qubits and the gate qubits, and increase the error of the two-qubit gates [7]. Zajac et al. [39] proposed that applying a dynamical compensation pulse between the qubits with crosstalk can effectively reduce the parallel error of the fixed-frequency qubit two-qubit gates. After simulation, we find that this scheme is also applicable to the two-qubit gates of tunable qubits and tunable coupling systems.

At the software level, Murali et al. [25] proposed a multi-objective optimization algorithm that minimizes the objective function of decoherence and crosstalk. The article uses z3 optimizer to search the minimum [9]. However, the z3 solver used in this solution has a very high computational complexity. Ding et al. [10] proposed a graph coloring based dynamical frequency allocation scheme. Interaction relationship between qubits and gates on the chip can be abstracted into a coupling

graph according to the coupling strength, so graph coloring algorithm can be used to avoid frequency collision. But this paper needs to allocate interaction frequencies according to each parallel situation of the algorithm, which means that a qubit needs multiple noise insensitive frequencies. The state-of-art magnetic flux control tunable qubits don't support such frequency-flux control relationship. Hua et al. [14] proposed a graph coloring based gate scheduling scheme. But this paper assumes that the execution time of two-qubit gates is the same at the compilation stage, which will cause unwanted parallelism between crosstalk gates. Xie et al. [37] proposed a co-optimizing pulses and scheduling solution for microwave-driven two-qubit gate chip. This scheme requires a global optimization of the gate control pulse, which is very difficult in the actual chip control system.

We propose a Optimizing Qubit Mapping and Gate Scheduling for Crosstalk Mitigation and Decoherence Suppression (OQMGS) scheme for tunable couplers and tunable qubits. Our scheme has high practicality and compatibility with actual quantum chips. Firstly, we migrate the compensation pulse scheme in [39] to the tunnable qubit tunnable coupler structure. Although the compensation scheme can cutoff the crosstalk, the global optimization of pulse parameters is intractable, we can only optimize the pulses of parallel gates in a small part of the chip. Therefore we have to divide the chip into small blocks where two-qubit gates can be executed parallelly.

Secondly, we introduce a compilation framework which consists of two steps. The first step is a mapping scheme that considers crosstalk. In order to mitigate the problem of crosstalk not being suppressed when only considering the decoherence error, our mapping scheme will search for a mapping that can simultaneously shorten the program execution time and mitigate crosstalk, i.e., using a heuristic cost function that maps the parallel gates within small blocks that are not neighbor to each other. The gates within small blocks can be executed parallelly because of the compensation pulse. Since the first step is a heuristic algorithm, we cannot find the exact optimal solution, so the crosstalk problem cannot be completely eliminated. Therefore, we introduce the second step, which is a gate scheduling scheme based on finding the maximum-independent set problem in graph theory. We abstract the crosstalk relationship between gates into a crosstalk graph model, and solve the maximum-independent set problem to select the largest set of crosstalk free quantum gates. We use this scheme to parallelize as many two-qubit gates as possible, and shorten the execution time of the quantum program under the premise of mitigating crosstalk.

The main contributions of this paper are as follows:

- We have migrated a pulse compensation crosstalk cutoff scheme used in the adiabatic gate system to a tunable coupling, tunable qubit system, and verified its effectiveness through simulation. The compensation pulse can reduce the error caused by crosstalk by up to two orders of magnitude.

- We propose a scheme that can simultaneously mitigate the crosstalk of spectator qubits and gate parallelism and shorten the execution time of quantum circuits.
- Our scheme uses appropriate pruning methods to compress the search space of the optimization algorithm, and save a lot of time compared with the IBM crosstalk compilation scheme based on the z3 optimizer.

II. PRELIMINARY

A. Basic Information

1) *Qubit*: Qubit is the basic unit of quantum information, which is a linear superposition of two basis states $|0\rangle$, $|1\rangle$, eq. (1)

$$|\psi\rangle = \alpha|0\rangle + \beta|1\rangle, |\alpha|^2 + |\beta|^2 = 1. \quad (1)$$

For a $n > 1$ -qubit quantum computer, its quantum state is a linear superposition over all 2^n computational basis states, eq. (2)

$$|\psi_n\rangle = \sum_{q_1 \cdots q_n \in \{0,1\}^n} c_{q_1 \cdots q_n} |q_1 \cdots q_n\rangle, \sum_{q_1 \cdots q_n} |c_{q_1 \cdots q_n}|^2 = 1. \quad (2)$$

2) *Gate*: The implementation of quantum computing is to use a series of quantum gates to perform unitary transformations on qubits $U|\psi\rangle$. The quantum gates are single-qubit gates such as RX gate and two-qubit gates such as CZ gate.

$$RX = \begin{pmatrix} 0 & 1 \\ 1 & 0 \end{pmatrix} \quad CZ = \begin{pmatrix} 1 & & & \\ & 1 & & \\ & & 1 & \\ & & & -1 \end{pmatrix} \quad (3)$$

3) *Quantum Circuit*: Quantum programs is represented by a gate-level quantum circuit fig. 1(a). Each line represents a qubit, and the quantum gates arranged in order on the line represent these gates acting on the target qubit in sequence. The final square represents the measurement. And a quantum circuit can also be represented by a Directed Acyclic Graph(DAG) $\mathcal{D}(q, g, e)$ fig. 1(b) where q is the set of qubits, g is the list of gates, and e is the dependencies between gates. For two different gates $g_i, g_j \in g, i \neq j, (g_i, g_j) \in e$ means that g_j depends on the state of the qubit after the execution of g_i .

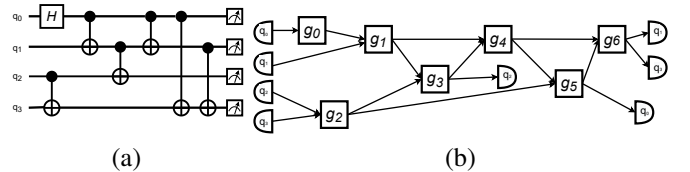


Fig. 1: (a) The circuit model of a quantum program example. (b) The DAG corresponding to the circuit in (a).

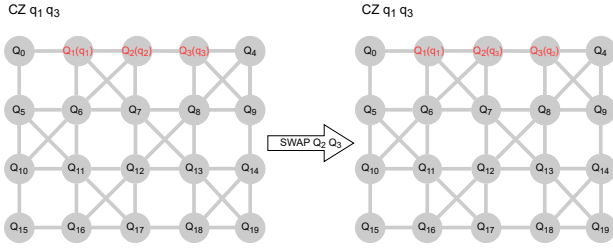


Fig. 2: IBM Q20 Tokyo coupling graph. The nodes are the physical qubits. Edges are couplers. $Q_i(q_j)$ means q_j is mapped to Q_i .

4) *Quantum Chip Coupling Structure*: Quantum chip's coupling structure can be considered as a coupling graph $\mathcal{G}(\mathbf{Q}, \mathbf{E})$, where \mathbf{Q} is the physical qubits and \mathbf{E} is the coupler set. IBM Q20 chip's coupling graph is shown in fig. 2 [28]. The qubits are placed on a planar geometry and couplers can only connect one qubit to its neighboring qubits. For example, Q_1 is connected to Q_2 and Q_7 through couplers, which means that a two-qubit gate can be applied on qubit Q_1, Q_2 and Q_1, Q_7 in either direction. However, Q_1 is not directly connected with Q_3 and we cannot apply a two-qubit gate on these two qubits directly. The qubits at the quantum program level are logical qubits q_i , and in the execution process, logical qubits need to be mapped to physical qubits Q_j on the actual chip $\pi : q_i \rightarrow Q_j$. Two-qubit gates can only be executed between qubits connected by a coupler. So the two-qubit gate CZ $q_1 q_3$ is executed after the swap $Q_2 Q_3$ is inserted [32].

B. Hardware Constraints of Superconducting Quantum Computing

1) Decoherence Noise and Tunable Qubit:

a) *Decoherence Noise*: Quantum systems are highly susceptible to external environmental influences, such as thermal noise, magnetic field fluctuations, etc. This effect will cause the loss of phase information of quantum states and the transition from high-energy levels to low-energy levels. This process is called decoherence [15].

Given a decoherence time T , the probability of decoherence of a qubit grows exponentially with time eq. (4).

$$P(t) = 1 - \exp\left(-\frac{t}{T}\right), \quad (4)$$

where $P(t)$ is the probability of decoherence of the qubit after time t . t is the elapsed time. T is the decoherence time, i.e. the time during which the qubit remains in a coherent state. In practical operations, qubits need to complete all computational tasks within the decoherence time, otherwise, the computed results may be erroneous.

b) *Tunable Qubit*: Qubit frequency is the transition energy from $|0\rangle$ to $|1\rangle$. In energy level diagram fig. 3(a), it is $\omega_q = \omega_{01} = E_1 - E_0$. The second excited state $|2\rangle$ has energy level E_2 . To prevent the leakage from $|0\rangle, |1\rangle$ to $|2\rangle$, there is an anharmonicity η s.t. $\omega_{12} = E_2 - E_1 = \omega_q + \eta$. Tunable qubit's frequency can be tuned by the external magnetic flux

Φ . There is a frequency spectrum in fig. 3(b). The decoherence time T is strongly related with the derivative $d\omega/d\Phi$. So there is a large range of the frequency call flux sensitive points has very short T for quantum computing. Because of the decoherence noise, the frequency tuning range is limited.

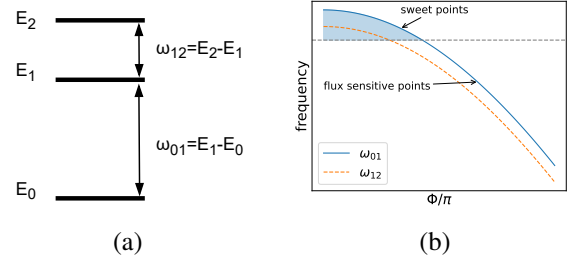


Fig. 3: (a) Qubit energy level. (b) The frequency spectrum for tunable qubits. The sweet points are the frequency range have long enough decoherence time while the flux sensitive points donnot.

2) *Tunable Coupler*: Current superconducting architectures use tunable couplers fig. 4 [2].

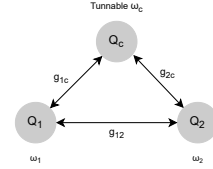


Fig. 4: Sketch of the tunable-coupling structure. The direct coupling strength between Q_1, Q_2 is g_{12} , and the ones between Q_i, Q_c are g_{1c}, g_{2c} , $g_{ic} > g_{12}$.

The Hamiltonian is as follows

$$\begin{aligned} H/\hbar = & \sum_{i=1,2,c} \omega_i a_i^\dagger a_i + \frac{\eta_i}{2} a_i^\dagger a_i^\dagger a_i a_i + \\ & g_{12}(a_1^\dagger - a_1)(a_2^\dagger - a_2) + \sum_{i=1,2} g_{ic}(a_i^\dagger - a_i)(a_c^\dagger - a_c). \end{aligned} \quad (5)$$

Where a_i, a_i^\dagger is the annihilation(creation) operator of qubit mode. g_{ij} is the coupling strength. When the frequency difference between the qubits and the coupler is large $|\Delta_{ic}| = |\omega_c - \omega_i| \gg g_{ic}$, the Hamiltonian can be transformed by the Schrieffer-Wolff(SW) transformation [5] into the following form,

$$H/\hbar = \sum_{i=1,2} \omega_i a_i^\dagger a_i + \frac{\eta_i}{2} a_i^\dagger a_i^\dagger a_i a_i + \tilde{g}_{12}(a_1^\dagger - a_2)(a_2^\dagger - a_1), \quad (6)$$

$$\tilde{g}_{12} = \frac{g_{1c}g_{2c}}{2} \left(\frac{1}{\Delta_{1c}} + \frac{1}{\Delta_{2c}} \right) + g_{12}, \Delta_{ic} = \omega_i - \omega_c. \quad (7)$$

In fig. 5(a) when ω_c is much larger than ω_i , because $\Delta_{ic} < 0$, \tilde{g}_{12} has a zero point. When executing a two-qubit gate, the frequencies of the qubits need to be tuned to the resonant

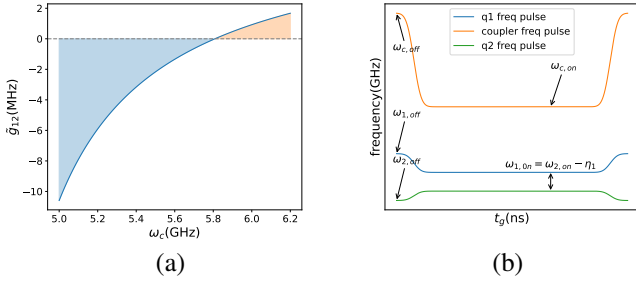


Fig. 5: (a) The relationship between \tilde{g}_{12} and the coupler frequency. There exists a coupler frequency where \tilde{g}_{12} is zero. When the coupler frequency decreases, the value of $|\tilde{g}_{12}|$ increases. (b) The dynamic gate pulse of q_1, q_2 and coupler c_{12} between q_1, q_2 . ω_i changed from $\omega_{i,off}$ to $\omega_{i,on}$, and $\omega_1 + \eta_1 = \omega_2$ is met. The coupler frequency was decreased from $\omega_{c,off}$ to $\omega_{c,on}$ to increase the \tilde{g}_{12} .

state, and at the same time, the c_{12} 's frequency needs to be tuned to the point where the equivalent coupling is larger in fig. 5(a), to ensure a fast gate execution time. In fig. 5(b), q_1, q_2 's frequencies satisfied $\omega_1 + \eta_1 = \omega_2$ [19] and the $|11\rangle$ and $|02\rangle$ states are resonant, after a period of time, the $|11\rangle$ state can acquire a π phase $|11\rangle \xrightarrow{e^{i\pi/2}} i|02\rangle \xrightarrow{e^{i\pi}} -|11\rangle$, thus we realize the CZ gate.

3) *Crosstalk & Compensation Pulse*: The qubit frequencies are tuned apart from resonant to mitigate the unwanted residual interactions, i.e. $|\Delta_{12}| \gg \tilde{g}$. The Hamiltonian eq. (5) can be written as the following form [20], [42].

$$H = \sum_n \tilde{E}_n |n\rangle, n \in \{0, 1\}^2, \tilde{E}_n = E_n + \Delta E_n, \quad (8)$$

$$\xi = \tilde{E}_{11} - \tilde{E}_{01} - \tilde{E}_{10} + \tilde{E}_{00}, \quad (9)$$

eq. (9) is called the ZZ coupling which is caused by energy level pushing. ZZ coupling is a commonly used metric of crosstalk strength. For a tunable coupling system, the coupler frequency $\omega_{c,off}$ will be set at the minimum of ZZ coupling, where the interaction between qubits is minimal [41].

Now we consider a physical model fig. 6(a). q_1, q_2 are gate qubit and their frequencies are tuned to the resonant frequency. q_s is a spectator qubit has residual interaction with q_1, q_2 . When there is no two qubit gates being executed, $\omega_{c,off}$ between q_2, q_s is set to the ZZ coupling minimum. If a CZ gate in fig. 6(a) is about to execute, q_1, q_2 are tuned to resonant, the ZZ crosstalk minimum will fail.

In fig. 6(a), the frequencies of q_1, q_2 are tuned to resonant frequency. In principle, we need to tune the frequency of the q_s far enough to avoid the near-resonant region. However, the narrow frequency range of qubits also brings out another problem. When the difference between $\omega_{q,on} - \omega_{q,off}$ is large, the two-qubit gate will be affected by pulse distortion [17]. Assuming that a single-qubit gate frequency of a qubit is $\omega_q = \omega_1$, the qubit frequencies around it will be roughly located around a frequency $\omega_n \in \omega_2 \pm \delta$ where $|\omega_2 - \omega_1| < \Delta_{dist}$, otherwise,

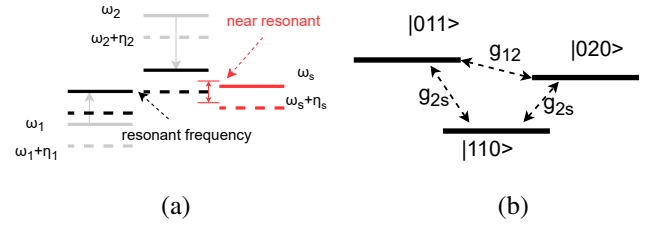


Fig. 6: (a) Sketch of the gate qubit q_1, q_2 and spectator qubit q_s energy level model. $\omega_1, \omega_2 + \eta_2$ are resonant, while the ω_s of spectator is also near the resonant frequency. (b) The sketch of the state interaction. The qubit order is $|q_s q_2 q_1\rangle$.

the neighboring qubit with large frequency difference will cause pulse distortion. Therefore, q_1, q_s , the neighbor of q_2 have similar frequencies as in fig. 6(a) and q_2 is likely to locate in near-resonant region of the two-qubit gate resonant frequency. We call this **frequency crowding**. As in fig. 6(b), during CZ execution, $|011\rangle, |020\rangle$ will oscillate to each other with coupling strength g_{12} . Because the spectator qubit is in the near-resonant region, the two-excitation state $|110\rangle$ also interacts with the states involved in the CZ interaction with coupling strength g_{2s} .

Zajac et al. [39] find that giving a dynamical compensation pulse to the coupler between spectator qubit and gate qubit as fig. 7 can minimize the residual stray couplings. They discuss the fixed-frequency qubit adiabatic gate system in their paper. Although our system is a tunable qubit two-qubit gate, the compensation has a same crosstalk cutoff effect in our simulation results.

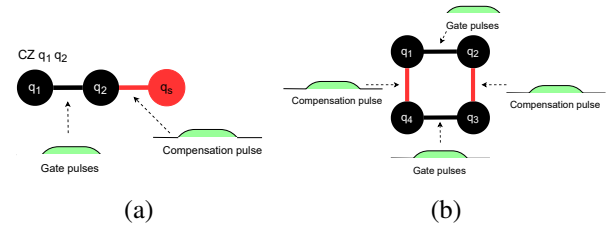


Fig. 7: (a) Illustration of the compensation scheme. During a gate between q_1, q_2 , we apply a small pulse to c_{2s} between q_2, q_s . The frequency of c_{2s} is changed from the ZZ minimum to a new frequency which can cut off the spectator qubit crosstalk. (b) Illustration of the compensation scheme of parallel two-qubit gate execution. Similarly, a small pulse to c_{14} and c_{23} that change their frequencies is used to cut off the parallel gate crosstalk.

In fig. 8(c), we set $\omega_{c,off}$ to the ZZ minimum when there is no CZ being executed. In fig. 8(a), the ZZ minimum frequency is not the frequency corresponding to the gate error minimum. While in fig. 8(b), the leakage minimum between $|110\rangle, |011\rangle$ and $|110\rangle, |020\rangle$, is the gate error minimum. So it is necessary to retune the coupler frequency between the spectator qubit and the gate qubit to achieve a new crosstalk cutoff frequency. Therefore, from fig. 8, the compensation

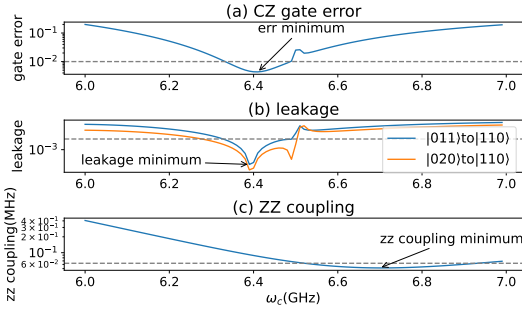


Fig. 8: (a) The relationship between the two-qubit gate error and the coupler frequency. (b) The relationship between the leakage and the coupler frequency. The qubit order is $|q_s q_2 q_1\rangle$. (c) The relationship between the ZZ coupling and the coupler frequency.

pulse is a dynamically bias that tune the coupler frequency to the near leakage minimum.

C. Constraints

Due to the limitation of physical system, an optimal qubit mapping and gate scheduling compilation scheme is necessary. Here we introduce the qubit mapping constraints and the gate time scheduling constraints based on physical background.

1) *Interconnection Constraint*: Each two-qubit gate needs to satisfy

$$D(\pi(g.q_1), \pi(g.q_2)) = 1 \quad (10)$$

D is the distance function of the qubit on the chip. $\pi(q_i)$ is the mapping of the qubit q_i . eq. (10) means that logical qubits should be mapped to those physical qubits that are coupled by couplers.

2) *Parallel Constraint*: To achieve the highest fidelity, the quantum gate parameters need to be optimized [30]. We focus on the two-qubit gates here. Based on the previous section section II-B3, in addition to the coupler and qubit parameters of the gate, we also need to optimize the coupler compensation pulse parameters between the gate qubits and the spectator qubits. Initially, we assume that all the spectator qubits around the gate qubits are at the single-qubit frequency and optimize the pulse parameters of each gate and all the couplers around it.

Due to the frequency crowding problem, in fig. 9(b) the single-qubit gate frequencies of Q_1, Q_3, Q_4 are close to each other. When they do not execute two-qubit gates, the coupler cutoffs the crosstalk by the ZZ minimum. But if two-qubit gates are executed, as shown in fig. 9(a), because of the narrow frequency range, the interaction frequency of the two-qubit gate is likely to be in the near-resonant region. At this time, the coupler c_{23} has to cutoff the interaction between Q_1, Q_2, Q_3 and Q_2, Q_3, Q_4 at the same time, similarly, c_{24} has to cutoff the interaction between Q_2, Q_3, Q_4 and Q_2, Q_4, Q_5 . Consequently, each group of near-resonant qubits' crosstalk involves multiple couplers, and each coupler is responsible for the crosstalk cutoff of multiple groups of near-resonant

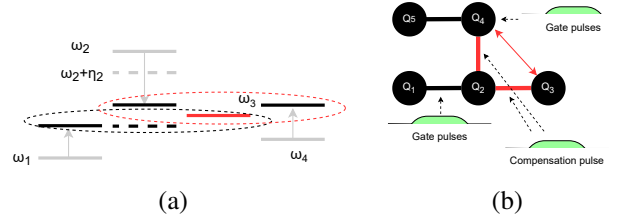


Fig. 9: (a) The interaction sketch of multiple spectator qubits. If Q_1, Q_2 and Q_4 are tuned to the interaction frequencies, Q_3 will participate in the interactions among Q_1, Q_2, Q_3 and Q_4, Q_2, Q_3 . (b) The compensation pulse of c_{23} should cutoff the crosstalk between Q_1, Q_2, Q_3 and Q_4, Q_2, Q_3 , and c_{24} Q_2, Q_3, Q_4 and Q_2, Q_4, Q_5 .

qubits. If the other qubits and gate parallelism on the chip are taken into account, the number of couplers that need to be optimized simultaneously will increase, the optimization of the compensation pulse will gradually spread to the global optimization of the chip. In addition, for a chip with $N \times N$ qubits, there are $2N(N-1)$ couplers, so the number of cases for executing two-qubit gates in parallel is $O(2^{N^2})$. Optimizing the compensation pulse is a intractable global optimization problem on the chip.

An alternative way is re-optimizing every $m \times n$, ($m, n < N$) qubit block on the chip fig. 10. Every parallel situation will be considered in the block and thus every two-qubit gates are allowed to execute in parallel in these small blocks. If different two-qubit gates are about to execute, they need to be mapped to physical qubits within a block. Otherwise, they need to have a certain distance on the chip to ensure that the spectator qubits outside the block are work at the single-qubit frequencies.

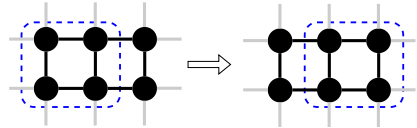


Fig. 10: The qubits and coupler in the blue block is re-optimized for every parallel execution situation. Shift the qubit blocks, so that every $m \times n$, ($m = n = 2$) block in the chip can execute any parallel two-qubit gate.

Based on this idea, the parallel constraint is that, given the maximum re-optimization block $m \times n$. If a set of gate g overlap in time

$$\forall g_i, g_j \in \mathbf{g}, (g_i.t, g_i.t + t_{g_i}) \cap (g_j.t, g_j.t + t_{g_j}) \neq \emptyset, \quad (11)$$

where t_g is the duration of g , $g.t$ is the execution starting time of g . Gate qubits should be mapped to the physical qubits within blocks that are not neighbor to each other. Suppose the allowed maximum parallel block is $m \times n$, the graph diameter of the parallel block is $m + n - 2$. Given a map π , we define a subset $Q_g = \{\pi(q) | \forall g \in \mathbf{g}, q \in g.q\}$ of all physical qubits Q , and obtain a subgraph \mathcal{G}_g of \mathcal{G} that only contains Q_g .

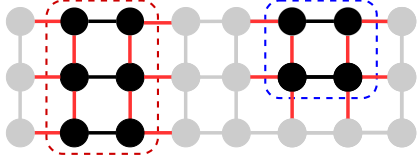


Fig. 11: Assume that the block size is 2×2 , the two-qubit gates mapped to the blue box satisfy the constraint. The diameter of the blue box is $d_g = 2 \leq 2$. And the two-qubit gates mapped to the red box violate the constraint, $d_g = 3 > 2$.

For a maximum parallel block with size $m \times n$, the maximum parallel block constraint can be transformed to

$$\max(d_g) \leq m + n - 2, \quad (12)$$

where d_g is the graph diameter of all the connected subgraph of \mathcal{G}_g . Otherwise, the gate time $g.t$ should be delayed to mitigate crosstalk.

III. QUBIT MAPPING & GATE SCHEDULING

In this section, we will introduce our compilation scheme step by step to illustrate how our design overcome the crosstalk and decoherence problem.

A. Crosstalk Mitigation Mapping

a) *Distance matrix*: Given a coupling graph $\mathcal{G}(\mathbf{Q}, \mathbf{E})$ of a quantum chip, we first compute the shortest path between every qubit pairs to obtain the distance matrix $D(\cdot, \cdot)$. The qubit pairs connected by couplers has distance 1.

b) *DAG and Top Layer*: We use DAG $\mathcal{D}(\mathbf{g}, \mathbf{e})$ to represent the execution constraints between quantum gates. The top layer F is the set of gates which have no unexecuted predecessors in the DAG. These gates can be executed instantly from a software perspective. A quantum gate, e.g., $CZ(q_i, q_j)$ can be placed in the set F when all previous gates on q_i, q_j have been executed.

c) *Gate Duration*: In this approach we should also take gate duration into consideration because crosstalk will happen in situation that multiple gate execution time overlap. The gate dependency of DAG \mathcal{D} cannot fully determine the timing of the gate. For example swap gate is consist by three CZ operations, swap gate duration is three times longer that CZ. If a list of gates about to execute is

$$\begin{aligned} &1^{\text{st}} \text{ SWAP}(q_i, q_j), (0, 3t_{CZ}), \\ &2^{\text{nd}} \text{ CZ}(q_m, q_n), (0, t_{CZ}), \\ &3^{\text{rd}} \text{ CZ}(q_m, q_l), (t_{CZ}, 2t_{CZ}) \quad l \neq i, j, n. \end{aligned} \quad (13)$$

We can see that $\text{SWAP}(q_i, q_j), \text{CZ}(q_m, q_l)$ have time overlap. On the contrary, keep the gate dependency of eq. (13) unchanged but change the first gate to $\text{CZ}(q_i, q_j)$, its execution time interval is $(0, t_{CZ})$ and there is no time overlap between the $1^{\text{st}}, 3^{\text{rd}}$ gates.

d) *Tree Search*: Suppose the map during time interval (t_1, t_2) is π , if we insert swap operation, for simplicity, written as s , we will get a new map in time $t > t_2 + t_s$. We define a swap based searching tree $\Psi(\pi, \mathcal{S})$, where π is the set of maps and \mathcal{S} is all possible swap operations. For $\pi_1, \pi_2 \in \pi$, $(\pi_1, \pi_2) \in \mathcal{S}$ if and only if

$$\begin{aligned} &\exists s(q_1, q_2) \in \mathcal{S}, \quad (14) \\ &\pi_1(q_1) = \pi_2(q_2) \cap \pi_1(q_2) = \pi_2(q_1) \cap \pi_1(q) = \pi_2(q) \forall q \neq q_1, q_2. \end{aligned} \quad (15)$$

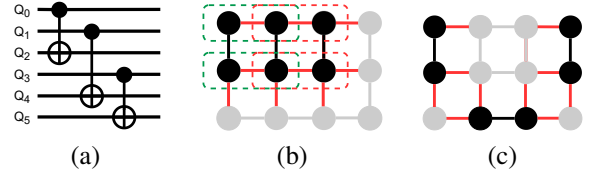


Fig. 12: (a) Circuit with three two qubit gates. (b, c) are two mapping on the chip. (b) Compensation pulses for the coupler in green boxes and red boxes need to be optimized. Otherwise, the these three gates' error will be dramatically increased by crosstalk. (c) The mapping of these three gates are far enough from each other and they immuned from crosstalk.

1) *Algorithm*: This algorithm based on the idea that the number of parameters to be re-optimized is highly related to the mapping state. In fig. 12(a), there are three two-qubit gates about to execute. fig. 12(b) and (c) are two mapping state. In fig. 12(c) all the spectator qubits are in idle state or executing single-qubit gate, so the compensation pulses optimized in the initialization stage are valid. While in fig. 12(b) three two-qubit gates are mapped to qubits that are close to each other, The spectator qubits in this situation are also executing two-qubit gates, and the compensation pulses need to be re-optimized.

a) *Overview*: The algorithm 1 shows the overview of crosstalk mitigation mapping. The algorithm first initializes a random initial map π_0 that assigns logical qubits to physical qubits, creates an empty DAG \mathcal{D}_o to store the output circuit. The algorithm iterates over the remaining gate set g in \mathcal{D} until it is empty. For each iteration, it calls a function searchForward that searches for a subset of gates g_{exc} that can be executed with minimal noise, given the current map π_l , the input DAG \mathcal{D} , the search depth L and the search width W . The search depth and width control how many gates and how many possible maps are considered in the search, respectively. It removes the gates g_{exc} from the input DAG \mathcal{D} and adds them to the output DAG \mathcal{D}_o . Finally, it updates the current map π_l by applying any swap gates in g_{exc} that are used to change the qubit layout for better error mitigation.

b) *Recursive Searching Forward*: The algorithm 2 is the details about function searchForward. algorithm 2 searches for a subset of gates that can be executed with minimal crosstalk noise, given a current map, an input DAG, a search depth and a search width. The function gets the top layer F of the input DAG, which is the set of gates that have no predecessors. It initializes an empty list g_{exc} to store the executable gates. It

Algorithm 1 crosstalk mitigation Mapping

Require: Coupling Graph $\mathcal{G}(\mathbf{Q}, \mathbf{E})$, DAG $\mathcal{D}(\mathbf{q}, \mathbf{g}, \mathbf{e})$, search depth L , search width W

Ensure: new DAG \mathcal{D}_o after compilation

```
1: get the remaining gate set  $\mathbf{g}$  in  $\mathcal{D}$ 
2: get a random initial map  $\pi_0$ 
3: let  $\mathcal{D}_o$  be a empty DAG
4: while  $\mathbf{g} \neq \emptyset$  do
5:   current map is  $\pi_l$ ,
6:    $g_{exc}$ =searchForward( $\pi_l, \mathcal{D}, L, W$ )
7:   remove the gates  $g_{exc}$  in  $\mathcal{D}$ 
8:   apply the gates  $g_{exc}$  to  $\mathcal{D}_o$ 
9:   for  $g$  in  $g_{exc}$  do
10:    if  $g$  in all possible swap set  $\mathbf{S}$  then
11:      apply  $g$  to  $\pi_l$  and get  $\pi_{l+1}$ 
12:       $\pi_l \leftarrow \pi_{l+1}$ 
13:    end if
14:  end for
15:  get the remaining gate set  $\mathbf{g}$  in  $\mathcal{D}$ 
16: end while
```

Algorithm 2 Function searchForward

Require: π_l, \mathcal{D}, L, W

Ensure: executable gates g_{exc}

```
1: get the top layer  $F$ 
2:  $g_{exc} = \emptyset$ 
3: add the  $g$  in  $F$  satisfied eq. (10) to  $g_{exc}$ 
4: remove  $g_{exc}$  from  $\mathcal{D}$ 
5: if  $L = 0$  then
6:   return  $g_{exc}$ 
7: end if
8: for  $s$  in  $\mathbf{S}$  do
9:   apply  $s$  to  $\pi_l$  and get  $\pi_{l+1}$ 
10:   $d \leftarrow \sum_{g \in F} D(\pi_{l+1}(g.q_1), \pi_{l+1}(g.q_2))$ 
11: end for
12: maxMapScore =  $-\infty$ 
13: for the first  $W$   $s$  in  $\mathbf{S}$  in ascending order  $d$  do
14:   apply  $s$  to  $\pi_l$  and get  $\pi_{l+1}$ 
15:    $g_{exc2}$  =searchForward( $\pi_{l+1}, \mathcal{D}, L - 1, W$ )
16:   mapScore  $\leftarrow$  scoreStep( $\pi_l, g_{exc} + s + g_{exc2}$ )
17:   if mapScore > maxMapScore then
18:      $g_{exc, best} \leftarrow s + g_{exc2}$ 
19:   end if
20: end for
21: return  $g_{exc} \leftarrow g_{exc} + g_{exc, best}$ 
```

adds the gates g in F that satisfy the condition in eq. (10) of the paper to g_{exc} . This condition checks if the logical qubits of g are adjacent in the coupling graph under the current map π_l . It removes g_{exc} from the input DAG \mathcal{D} . If the search depth L is zero, it returns g_{exc} and terminates the function. Otherwise, it iterates over all possible swap gates s in the set \mathbf{S} that can be applied to the current map π_l to change the qubit layout. For each swap gate s , it applies s to π_l and gets a new map π_{l+1} . It then calculates the distance sum d for the gates in F under the new map π_{l+1} . It initializes a variable maxMapScore to store the maximum score of a map. It iterates over the first W swap gates s in the set \mathbf{S} in ascending order of d , where W is the search width that controls how many possible maps are considered in the search. The reason for this is that we choose the s that shorten the distance between gate qubits. For each swap gate s , it applies s to π_l and gets a new map π_{l+1} . It then recursively calls the function searchForward with the new map π_{l+1} , the input DAG \mathcal{D} , the search depth $L - 1$ and the search width W . It gets a list of executable gates g_{exc2} from the recursive call. It calculates the score of the map π_{l+1} by calling a function scoreStep with the current map π_l and the list of gates $g_{exc} + s + g_{exc2}$. The function scoreStep is defined in algorithm 3 and it evaluates the map based on the crosstalk noise, the number of swap gates and the number of executable gates. If the score of the map π_{l+1} is greater than the maxMapScore, it updates the maxMapScore and stores the list of gates $g_{exc, best} = s + g_{exc2}$ as the best choice for the current iteration. After iterating over the first W swap gates, it returns the list of executable gates $g_{exc} + g_{exc, best}$ and terminates the function.

c) *Heuristic Scoring Strategy:* The algorithm 3 is a function that evaluates the score of a map, given a current map and a list of executable gates. It initializes a dictionary Q_t that stores the time of each physical qubit \mathbf{Q} and sets it to zero for all qubits. It initializes an empty list layers to store the layers of gates that can be executed in parallel. It initializes a variable $|s|$ to store the number of swap gates in the list of executable gates g_{exc} . It iterates over the gates g in the list g_{exc} . If g is a swap gate, it applies g to the current map π and gets a new map π . For each layer in the list layers, it checks if the time interval of g overlaps with the time intervals of the gates in the layer, using the dictionary Q_t and the duration t_g of g . If there is an overlap, it gets the set of physical qubits \mathbf{Q}_g involved in the gates in the layer and g , and induces a subgraph \mathcal{G}_g from the coupling graph \mathcal{G} using the set \mathbf{Q}_g . If there is no connected subgraph of \mathcal{G}_g that violates the parallel constraint eq. (12), it updates the time of the physical qubit $\pi(g.q)$ by adding the duration t_g of g , and appends g to the layer. Otherwise, it sets the time of the physical qubit $\pi(g.q)$ to the maximum time of the physical qubits involved in the gates in the layer. Repeat and try to set g to the next layer in layers. If there is no layer for g , it creates a new layer with g and appends it to the list layers. It also sets the time of the physical qubit $\pi(g.q)$ to the maximum time in Q_t plus the duration t_g of g . After iterating over all the gates in g_{exc} , it gets the maximum time t_{end} in Q_t , which is the total execution

Algorithm 3 Function scoreStep

Require: π, g_{exc} **Ensure:** score

```

1:  $Q_t \leftarrow$  a dictionary with  $Q_t[Q] = 0, \forall Q \in \mathcal{Q}$ 
2: layers  $\leftarrow \square$ 
3:  $|s| \leftarrow$  the number of gate  $g \in \mathcal{S}$ 
4: for  $g$  in  $g_{exc}$  do
5:   if  $g \in \mathcal{S}$  then
6:     apply  $g$  to  $\pi$  and get a new  $\pi$ 
7:   end if
8:   for layer in layers do
9:     if time interval  $(Q_t[\pi(g.q)], Q_t[\pi(g.q)] + t_g)$  has
10:    overlap with the gates in layer then
11:       $Q_g \leftarrow \{\pi(g_l.q) | \forall g_l \in \text{layer} \cup g\}$  and induce  $\mathcal{G}_g$ 
12:      from  $Q_g$  and  $\mathcal{G}$ 
13:      if there is not connected subgraph of  $\mathcal{G}_g$  violate
14:      the parallel constraint then
15:         $Q_t[\pi(g.q)] \leftarrow Q_t[\pi(g.q)] + t_g$ 
16:        layer.append( $g$ )
17:      else
18:         $t \leftarrow$  the maximum  $Q_t[\pi(g_l.q)]$  for gate qubits
19:         $g_l.q$  in layer
20:         $Q_t[\pi(g.q)] \leftarrow t$ 
21:      end if
22:    end if
23:    if there is no layer for  $g$  then
24:      layers.append( $[g]$ )
25:       $t \leftarrow$  the maximum time in  $Q_t$ 
26:       $Q_t[\pi(g.q)] \leftarrow t + t_g$ 
27:    end if
28:  end for
29:  $t_{end} \leftarrow$  the maximum time in  $Q_t$ 
30: score =  $\frac{|g_{exc}| - 3|s|}{t_{end}}$ 
31: return score

```

time of the gates in g_{exc} . It calculates the score of the map as the ratio of the number of executable gates minus three times the number of swap gates, divided by the total execution time. It returns the score and terminates the function.

d) Key Design: Our key design is that, algorithm 3 will delay the gate execution time when the parallel constraint eq. (12) is violated. When the mapping state found by the search tree has severe crosstalk, the extended execution time as a loss function will penalize this strategy, so that we can find a mapping strategy that minimizes both decoherence noise and crosstalk noise.

e) Complexity Analysis: The complexity of algorithm 3 depends on the number of iterations of the gate set $|g|$ and the number of layers L . Therefore, the time complexity can be expressed by the product of these two factors $O(|g|L)$. The most expensive operation is the recursive call in algorithm 2. The algorithm makes at most W recursive calls, each with a reduced depth of $L - 1$. Therefore, the time complexity can

be expressed by the recurrence relation:

$$\begin{aligned}
T(L, W) &= WT(L - 1, W) + O(W|g|L), \\
&= W^L T(0, W) + O\left(\sum_{l=0}^{L-1} W^l |g|L\right), \\
&= O(W^L(|g|L + 1)). \tag{16}
\end{aligned}$$

Where $|g|$ is the gate number in \mathcal{D} . If algorithm 1 calls the searchForward function at most $|g|$ times, once for each gate in the original DAG. Therefore, the time complexity can be expressed by the product $O(|g|W^L(|g|L + 1)) = O(W^L|g|^2L)$, which is only polynomial to the circuit scale $|g|$.

B. Maximum-Independent Set-Based Gate Scheduling

Since the mapping algorithm is heuristic, it cannot completely guarantee to suppress the gate time delay problem caused by parallel constraint. In this case, a gate execution order that minimizes the algorithm execution time needs to be chosen. Therefore, we need to schedule gates in a layer to improve circuit's parallelism.

a) Crosstalk Graph: First, we introduce the crosstalk graph $\mathcal{T}(g, \mathbf{X})$, where the nodes g are two-qubit gates that are executed in parallel in the same layer. If there is crosstalk effect between the nodes or the gate qubits are mutually spectator qubits, then there is an edge $x \in \mathbf{X}$ between the nodes.

$$\begin{aligned}
\min(D(\pi(g_1.q), \pi(g_2.q))) &= 1, \\
\Rightarrow (g_1, g_2) &\in \mathbf{X}, \tag{17}
\end{aligned}$$

eq. (17) means that if the logical qubits of two two-qubit gates are mapped to the physical qubits on the chip with a minimum distance of 1, there is crosstalk between the gates.

1) Algorithm:

a) Divide Gates into Sub-layers: The algorithm 4 takes DAG $\mathcal{D}(q, g, e)$ as input, and a coupling graph $\mathcal{G}(Q, E)$ that represents the connectivity of the qubits on the quantum hardware. The algorithm outputs the gate time for each gate in the circuit, which is the start and end time of the gate execution. It first calls a function extractGateTime to assign a default gate time for each gate in the circuit, based on predefined gate durations. Suppose the ancestor of g 's execution time is $(g_{ancestor}.t, g_{ancestor}.t + t_{g_{ancestor}})$ then g will execute at $(g.t, g.t + t_g)$. It then creates an empty list of layers, where each layer is a set of gates that can be executed in parallel without violating the hardware constraints eq. (10) or the circuit dependency. It iterates over all the gates in the circuit, and for each gate, it tries to find a layer that has execution time overlap with the gate. If such a layer exists, it adds the gate to that layer. Otherwise, it creates a new layer with the gate as the only element. It then calls a function generatePartition to partition the layers into sub-layers, such that each sub-layer contains gates that can be executed in parallel. It then adds barriers to the gates in each layer according to the partition, to ensure that the gates in different sub-layers are executed

sequentially. The two-qubit gates in fig. 13(a) can be executed parallelly, but due to the barrier, the second CZ_{q_2, q_4} depends on barrier q_1, q_2, q_3 , it is delayed.

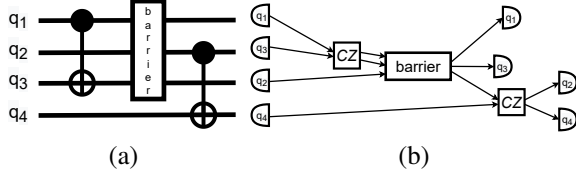


Fig. 13: (a) A barrier was inserted between these two two-qubit gates, and the order of the gates in the corresponding DAG (b) became as follows: $CZ_1 < \text{barrier} < CZ_2$.

It then calls the `extractGateTime` function again to update the gate time for each gate, taking into account the barriers. It then returns the gate time for each gate as the output of the algorithm.

Algorithm 4 Gate Scheduling Algorithm

Require: DAG $\mathcal{D}(q, g, e)$, Coupling Graph $\mathcal{G}(Q, E)$

Ensure: `gTime`

```

1: gTime ← extractGateTime( $\mathcal{D}$ )
2: layers ← []
3: for  $g$  in  $g$  do
4:   for layer in layers do
5:     if  $\exists q_l \in \text{layer}$  has execution time overlap with gTime[ $g$ ] then
6:       layer.append( $g$ )
7:     end if
8:   end for
9:   if there is no layer for  $g$  then
10:    layers.append([ $g$ ])
11:   end if
12: end for
13: partitions ← generatePartition(layers,  $\mathcal{G}$ )
14: for (partition, layer) in (partitions, layers) do
15:   add barrier to gates in layer according to partition
16: end for
17: gTime ← extractGateTime( $\mathcal{D}$ )
18: return gTime

```

b) Maximum-independent Set Partition: The algorithm 5 works by iterating over each layer and finding the crosstalk graph \mathcal{T} , which is a graph that represents the interference between the gates in the layer. The algorithm then tries to find the maximum-independent sets of \mathcal{T} , which are subsets of nodes that are not adjacent to each other.

In fig. 14(a), 6 gates are mapped to the chip, using the condition eq. (17), we can get the corresponding crosstalk graph fig. 14(b). The maximum-independent sets in fig. 14(b) are $[g_{q_1, q_2}, g_{q_5, q_6}, g_{q_{11}, q_{12}}]$, $[g_{q_3, q_7}, g_{q_9, q_{10}}]$, $[g_{q_4, q_8}]$.

A python library Networkx [13] provides a function `maxIndependentSet` that solve the maximum-independent set problem approximately in polynomial time. After calling the function, algorithm 5 assigns each node to a partition based on the

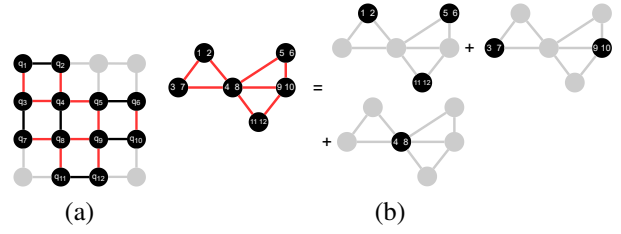


Fig. 14: (a) The parallel two qubit gates, the red edges is the coupler connecting gate qubits and spectator qubits. (b) The crosstalk graph, each node is the parallel gate in (a). The crosstalk graph is divided into three subgraph that each have no interconnection.

independent sets. Let's focus on line-9 to line-18, if the number of independent set is large, a layer will be divided into a long list of sub-layers, and the quantum circuit execution time is extended. Because we introduce a compensation pulse scheme migrated from Zajac et al. [39], the quantum chip control system allows a small block of re-optimization that allows the parallel execution. It is possible to find a partition that is not the maximum independent set, but the qubits corresponding to the parallel gates will not violate the parallel constraints eq. (12). Such partition have shorter list of sub-layer, i.e., shorter execution time, and immuned from crosstalk. To find such partition, we try to allocate the nodes in descending order degree to p partitions. If the constraint is violated after the allocation, the algorithm increases the number of partitions p until the parallel constraint is satisfied.

c) Complexity Analysis: The complexity of algorithm 5 is $O(|g||\mathcal{G}|)$, where $|\mathcal{G}|$ is the complexity of finding a maximum-independent set. The complexity of `maxIndependentSet` function in Networkx is $O(|\mathcal{G}|) = O(|g|/(\log^2 |g|))$ [13], [33], where $|g|$ corresponding to the node number of \mathcal{G} which is at most the number of gate. The algorithm 5 calls the `maxIndependentSet` function at most $|g|$ times. Because algorithm 4 calls the algorithm 5 once and the complexity of the loop and `extractGateTime` are $|g|^2$, the whole complexity is $O(|g|^2 + |g||\mathcal{G}|) = O(|g|^2(1/(\log^2 |g|) + 1)) = O(|g|^2)$

IV. EVALUATION

A. Baseline

In this section, we evaluate our OQMGS algorithm and compare them with the following baselines:

a) Mapping without Crosstalk Mitigation: Several recent algorithms proposed by IBM [40], Venturelli et al. [34], Zulehner et al. [43] and Li et al. [22] try to solve the mapping problem. Among them, Li's Sabre beats the others in the performance of benchmarkings, we use it as baseline in this paper.

b) Crosstalk Mitigation Mapping Baseline: Murali et al. [25] proposed a software scheme to mitigation crosstalk. Hua et al. [14] proposed a Crosstalk-Aware Compilation Framework (CQC). They are used for comparison in this paper.

Algorithm 5 function generatePartition

Require: layers, Coupling Graph $\mathcal{G}(Q, E)$ **Ensure:** partitions is a dictionary which partitions[g] = i which means that g is in the i^{th} partition

```
1: for layer in layers do
2:   get the crosstalk graph  $\mathcal{T}$  from the gates in layer
3:    $p = 2$ 
4:   while the partitions violates the parallel constraint do
5:     independentSets  $\leftarrow$  maxIndependentSet( $\mathcal{T}$ )
6:     if number of independentSets larger than  $p$  then
7:        $i = 0$ 
8:       for node in  $\mathcal{T}$  in descending order do
9:         partitions[node] =  $i \bmod p$ 
10:         $i \leftarrow i + 1$ 
11:      end for
12:    else
13:       $i = 0$ 
14:      for set in independentSets do
15:        partitions[node] =  $i$  for node in set
16:         $i \leftarrow i + 1$ 
17:      end for
18:    end if
19:     $p \leftarrow p + 1$ 
20:  end while
21: end for
22: return partitions
```

B. Architectural Features

We consider a chip architecture with 2D grid of $N \times N$ frequency tunable couplers and qubits. The frequency range of qubit is $\omega_q \in (4, 5)$ GHz. The frequency range of coupler is $\omega_c \in (5, 7)$ GHz. The anharmonicity of coupler and qubit is $\eta \approx 200$ MHz. The coupling strength $g_{ic} \approx 100$ MHz, $g_{12} \approx 10$ MHz. Qubits are connected by flux-tunable couplers, with its own independent external magnetic flux control. Last but not least, the initial error and measurement error are both set to be 0.01 ± 0.001 . These parameters are set to realistic values in line with experimental data from the literature [16].

C. Benchmark

To evaluate our algorithm, we select the benchmark circuits from the IBM qiskit [8]’s Github and Revlib [36]. Additionally, to verify the effect of the compensation pulse on reducing the crosstalk on the gate fidelity, we used the interleaved RB scheme [23].

D. Simulation of Interleaved RB

As shown in fig. 15, we simulated two interleaved RB, where two-qubit gates and random Clifford gates were repeated on q_1, q_2 on a 1×3 chip, while giving the spectator qubit a pulse to dynamically tune its frequency, which is equivalent to the spectator qubit performing two-qubit gates in parallel with the other qubits. In the fig. 15(a), the coupler between the spectator qubit and the gate qubit did not have

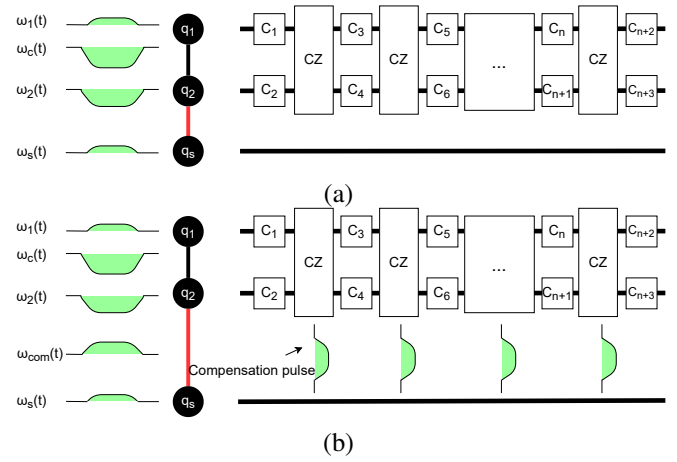


Fig. 15: (a) The sketch of interleaved RB, $\omega_1(t), \omega_c(t), \omega_2(t)$ are the gate pulse of CZ q_1, q_2 , $\omega_s(t)$ is the spectator qubit’s frequency pulse. (b) The compensation pulse $\omega_{com}(t)$ is performed between q_2, q_s whenever the CZ gate is executing.

a compensation pulse, while in fig. 15(b), the spectator qubit and the gate qubit had a compensation pulse.

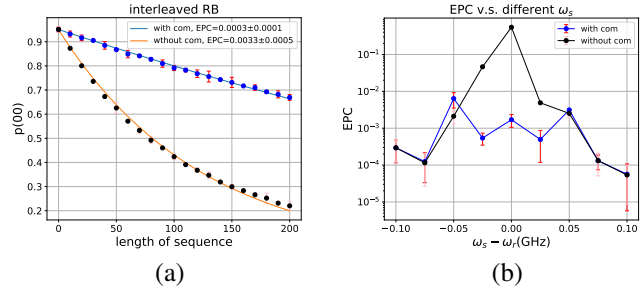


Fig. 16: (a) Interleaved RB result. The Error Per CZ (EPC) with compensation is 0.0003 ± 0.0001 and the one without is 0.0033 ± 0.0005 . The detune between resonant frequency and frequency is $|\omega_s - \omega_r| = 0.02$ GHz (b) Perform the interleaved RB at different $\omega_s(t)$. Increase of EPC near resonant can be greatly reduced by compensation pulse.

From fig. 16(a), it can be seen that the result obtained by interleaved RB is that the gate error with compensation pulse is 1/10 of the one without compensation pulse. In fig. 16(b), the gate error mainly increases when the spectator qubit is near the resonant frequency, and adding compensation pulse can reduce the error by nearly two orders of magnitude.

E. Compilation Time

If the compilation complexity is intractable, the advantage of quantum computing will be invalidated. Therefore, we first compare the time complexity of the baselines.

In fig. 17, among the four baselines, the crosstalk-aware schedule scheme in the IBM qiskit library requires at least exponential increase in compilation time as the quantum program scale increases. Because our scheme uses L, W as maximum searching scale to prune the searching tree, our

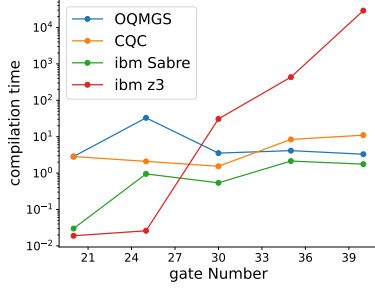


Fig. 17: The compilation time of four schemes with respect to the circuit gate number.

scheme maintains the compilation time at the order of $O(10^1)$ s as the quantum program scale increases, and have strong scalability. The reason for the exponential time requirement is that the IBM schedule scheme convert the problem to a Satisfiability Modulo Theories(SMT) problem, which is NP-hard. In the subsequent comparison, since the crosstalk-aware schedule scheme of IBM qiskit has requires extremely high time complexity and cannot be truly applied to the compilation, we won't consider this baseline in the following section.

F. Fidelity

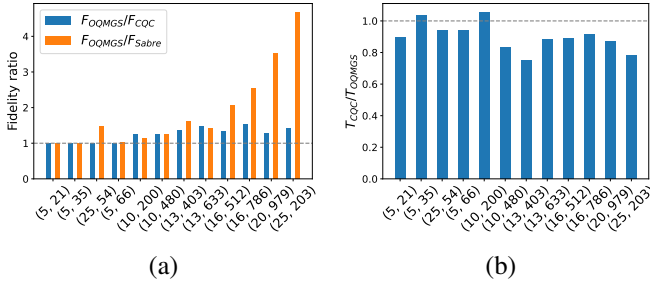


Fig. 18: (a) The x label in the figure is (N_Q, N_G) N_Q is the number of qubits, N_G is the number of gates, representing the scale of the circuit. y label is the fidelity ratio. (b) The ratio of execution time T_{OQMGs}/T_{CQC} with respect to the circuit scale.

Circuit fidelity has been proved to be significant for the quantum computer in NISQ-era. We used Aer, the noise quantum circuit simulation module of qiskit [8] to show the OQMGs's ability to maintain the fidelity. As shown in fig. 18(a), when the circuit scale is small, the number of gates is less than 100, corresponding to 4mod5-v1_22, etc., the fidelity difference of the three schemes is not large. When the circuit scale reaches three to four hundred gates, corresponding to qft and ising model, multiplier_n25 and other quantum circuits, our scheme and CQC have higher fidelity than Sabre because they consider crosstalk. OQMGs improve at most 4 times of fidelity compared to Sabre. In fig. 18(b) the execution time of OQMGs is shorten by the crosstalk

mitigation mapping. Therefore, our scheme has higher fidelity than CQC because our mapping scheme can both mitigate crosstalk and suppress decoherence error.

V. RELATED WORK

A. Mapping

There are many schemes for optimizing mapping without crosstalk consideration [34], [40], [43]. The current feasible schemes turn the mapping problem into a heuristic search problem [32], abstracting the swap gate as an edge connecting different mapping states [31], and using some function that reflects the length of the algorithm execution time to determine which swap operation should be selected [22].

B. Hardware Crosstalk Mitigation

Current solutions reduce crosstalk noise by qubit design [11], [21]; or to add compensation pulses between qubits [29], [35]. These schemes solve the crosstalk problem locally on the chip. However, if we want to solve the crosstalk between any qubits on the chip globally, we have to optimize the compensation pulses on all qubits simultaneously, which is a very difficult task.

C. Software Crosstalk Mitigation

Murali et al. [25] uses a multi-objective optimization scheme that considers both crosstalk and decoherence time, While from the article, this scheme cannot guarantee the complete elimination of crosstalk, and the z3 optimizer has a high algorithm complexity. Hua et al. [14] use a graph coloring scheme to schedule the gate timing, but only consider the crosstalk problem, and do not take both crosstalk and decoherence noise into account. Another solution is to mitigate crosstalk by qubit frequency allocation, Klimov et al [18] proposed a snake optimizer scheme which divides the frequency allocation problem to multiple greedy optimization problem. Ding et al. [10] uses a graph coloring scheme to dynamically allocate frequencies. By dynamically tuning the frequency, avoid frequency collisions, and thus mitigate crosstalk. However, when it comes to two-qubit gate frequency allocation, these scheme requires that the chip has multiple stable working frequencies, which is very difficult for frequency tunnable qubit, because the qubits that are not working on the sweet point have very short T_2 , and are easily affected by decoherent noise. Xie et al. [37] combine graph optimization and compensation pulses to optimize at the software and hardware levels, This scheme requires optimizing the pulse parameters for each step of execution, which is a difficult task for the control system. Moreover, this optimization algorithm cannot find the global optimal solution. It can not completely eliminate the crosstalk.

VI. CONCLUSION AND FUTURE WORK

In this paper, firstly, we have migrated the dynamic compensation pulse scheme for the adiabatic gate to the tunable coupling tunnable qubit system, and verified by simulation calculation that the compensation pulse can also turn off the

spectator qubit crosstalk and parallel crosstalk in this system. Secondly, we introduce a qubit mapping scheme that considers both the qubit decoherence time limit and the quantum chip crosstalk effect. Compared with previous mapping schemes, this scheme ensures that the parallel two-qubit gates mapped to the physical qubits have the lowest crosstalk effect. We also introduce a gate scheduling scheme based on the graph maximum-independent set model in graph theory. Experiments show that the combination of these two schemes is better than the CQC compilation framework. In addition, compared with the Sabre map scheme in the IBM qiskit library, our scheme has greatly improved fidelity. Compared with IBM's crosstalk-aware schedule scheme, the compilation time is greatly reduced. In the future, first, we will use experiments to verify the cutoff effect of our compensation pulse on the spectator qubit crosstalk, and second, we will apply our scheme to the real quantum circuit compilation.

REFERENCES

- [1] C. G. Almudever, L. Lao, X. Fu, N. Khammassi, I. Ashraf, D. Iorga, S. Varsamopoulos, C. Eichler, A. Wallraff, L. Geck *et al.*, "The engineering challenges in quantum computing," in *Design, Automation & Test in Europe Conference & Exhibition (DATE), 2017*. IEEE, 2017, pp. 836–845.
- [2] F. Arute, K. Arya, R. Babbush, D. Bacon, J. C. Bardin, R. Barends, R. Biswas, S. Boixo, F. G. Brandao, D. A. Buell *et al.*, "Quantum supremacy using a programmable superconducting processor," *Nature*, vol. 574, no. 7779, pp. 505–510, 2019.
- [3] A. Ash-Saki, M. Alam, and S. Ghosh, "Qure: Qubit re-allocation in noisy intermediate-scale quantum computers," in *Proceedings of the 56th Annual Design Automation Conference 2019*, 2019, pp. 1–6.
- [4] A. Ash-Saki, M. Alam, and S. Ghosh, "Analysis of crosstalk in nisq devices and security implications in multi-programming regime," in *Proceedings of the ACM/IEEE International Symposium on Low Power Electronics and Design*, 2020, pp. 25–30.
- [5] S. Bravyi, D. P. DiVincenzo, and D. Loss, "Schrieffer–wolff transformation for quantum many-body systems," *Annals of physics*, vol. 326, no. 10, pp. 2793–2826, 2011.
- [6] J. Bylander, S. Gustavsson, F. Yan, F. Yoshihara, K. Harrabi, G. Fitch, D. G. Cory, Y. Nakamura, J.-S. Tsai, and W. D. Oliver, "Noise spectroscopy through dynamical decoupling with a superconducting flux qubit," *Nature Physics*, vol. 7, no. 7, pp. 565–570, 2011.
- [7] J. Chu and F. Yan, "Coupler-assisted controlled-phase gate with enhanced adiabaticity," *Physical Review Applied*, vol. 16, no. 5, p. 054020, 2021.
- [8] A. Cross, "The ibm q experience and qiskit open-source quantum computing software," in *APS March meeting abstracts*, vol. 2018, 2018, pp. L58–003.
- [9] L. De Moura and N. Bjørner, "Z3: An efficient smt solver," in *International conference on Tools and Algorithms for the Construction and Analysis of Systems*. Springer, 2008, pp. 337–340.
- [10] Y. Ding, P. Gokhale, S. F. Lin, R. Rines, T. P. Propson, and F. T. Chong, "Systematic crosstalk mitigation for superconducting qubits via frequency-aware compilation," *2020 53rd Annual IEEE/ACM International Symposium on Microarchitecture (MICRO)*, pp. 201–214, 2020.
- [11] A. Finck, S. Carnevale, D. Klaus, C. Scerbo, J. Blair, T. McConkey, C. Kurter, A. Carniol, G. Keefe, M. Kumph *et al.*, "Suppressed crosstalk between two-junction superconducting qubits with mode-selective exchange coupling," *Physical Review Applied*, vol. 16, no. 5, p. 054041, 2021.
- [12] B. Foxen, C. Neill, A. Dunsworth, P. Roushan, B. Chiaro, A. Megrant, J. Kelly, Z. Chen, K. Satzinger, R. Barends *et al.*, "Demonstrating a continuous set of two-qubit gates for near-term quantum algorithms," *Physical Review Letters*, vol. 125, no. 12, p. 120504, 2020.
- [13] A. Hagberg and D. Conway, "Networkx: Network analysis with python," URL: <https://networkx.github.io>, 2020.
- [14] F. Hua, Y. Jin, Y.-H. Chen, C. Zhang, A. B. Hayes, H. Gao, and E. Z. Zhang, "Cqc: A crosstalk-aware quantum program compilation framework," 2022.
- [15] G. Ithier, E. Collin, P. Joyez, P. Meeson, D. Vion, D. Esteve, F. Chiarello, A. Shnirman, Y. Makhlin, J. Schrieffer *et al.*, "Decoherence in a superconducting quantum bit circuit," *Physical Review B*, vol. 72, no. 13, p. 134519, 2005.
- [16] M. Kjaergaard, M. E. Schwartz, A. Greene, G. O. Samach, A. Bengtsson, M. O'Keefe, C. M. McNally, J. Braumüller, D. K. Kim, P. Krantz *et al.*, "Programming a quantum computer with quantum instructions," *arXiv preprint arXiv:2001.08838*, 2020.
- [17] P. Klimov, J. Kelly, K. Satzinger, Z. Chen, H. Neven, and J. Martinis, "Optimizing quantum gate frequencies for google's quantum processors," *Bulletin of the American Physical Society*, vol. 65, 2020.
- [18] P. V. Klimov, J. Kelly, J. M. Martinis, and H. Neven, "The snake optimizer for learning quantum processor control parameters," *arXiv preprint arXiv:2006.04594*, 2020.
- [19] P. Krantz, M. Kjaergaard, F. Yan, T. P. Orlando, S. Gustavsson, and W. D. Oliver, "A quantum engineer's guide to superconducting qubits," *Applied physics reviews*, vol. 6, no. 2, 2019.
- [20] S. Krinner, S. Lazar, A. Remm, C. K. Andersen, N. Lacroix, G. J. Norris, C. Hellings, M. Gabureac, C. Eichler, and A. Wallraff, "Benchmarking coherent errors in controlled-phase gates due to spectator qubits," *Physical Review Applied*, vol. 14, no. 2, p. 024042, 2020.
- [21] J. Ku, X. Xu, M. Brink, D. C. McKay, J. B. Hertzberg, M. H. Ansari, and B. Plourde, "Suppression of unwanted z z interactions in a hybrid two-qubit system," *Physical review letters*, vol. 125, no. 20, p. 200504, 2020.
- [22] G. Li, Y. Ding, and Y. Xie, "Tackling the qubit mapping problem for nisq-era quantum devices," in *Proceedings of the Twenty-Fourth International Conference on Architectural Support for Programming Languages and Operating Systems*, 2019, pp. 1001–1014.
- [23] E. Magesan, J. M. Gambetta, B. R. Johnson, C. A. Ryan, J. M. Chow, S. T. Merkel, M. P. Da Silva, G. A. Keefe, M. B. Rothwell, T. A. Ohki *et al.*, "Efficient measurement of quantum gate error by interleaved randomized benchmarking," *Physical review letters*, vol. 109, no. 8, p. 080505, 2012.
- [24] D. Maslov, J.-S. Kim, S. Bravyi, T. J. Yoder, and S. Sheldon, "Quantum advantage for computations with limited space," *Nature Physics*, vol. 17, no. 8, pp. 894–897, 2021.
- [25] P. Murali, D. C. McKay, M. Martonosi, and A. Javadi-Abhari, "Software mitigation of crosstalk on noisy intermediate-scale quantum computers," in *Proceedings of the Twenty-Fifth International Conference on Architectural Support for Programming Languages and Operating Systems*, 2020, pp. 1001–1016.
- [26] C. Neill, P. Roushan, K. Kechedzhi, S. Boixo, S. V. Isakov, V. Smelyanskiy, A. Megrant, B. Chiaro, A. Dunsworth, K. Arya *et al.*, "A blueprint for demonstrating quantum supremacy with superconducting qubits," *Science*, vol. 360, no. 6385, pp. 195–199, 2018.
- [27] M. A. Nielsen and I. Chuang, "Quantum computation and quantum information," 2002.
- [28] S. Nishio, Y. Pan, T. Satoh, H. Amano, and R. V. Meter, "Extracting success from ibm's 20-qubit machines using error-aware compilation," *ACM Journal on Emerging Technologies in Computing Systems (JETC)*, vol. 16, no. 3, pp. 1–25, 2020.
- [29] W. Nuerbolati, Z. Han, J. Chu, Y. Zhou, X. Tan, Y. Yu, S. Liu, and F. Yan, "Canceling microwave crosstalk with fixed-frequency qubits," *Applied Physics Letters*, vol. 120, no. 17, p. 174001, 2022.
- [30] O. Shindi, Q. Yu, P. Girdhar, and D. Dong, "Model-free quantum gate design and calibration using deep reinforcement learning," *IEEE Transactions on Artificial Intelligence*, 2023.
- [31] M. Y. Siraichi, V. F. d. Santos, C. Collange, and F. M. Q. Pereira, "Qubit allocation," in *Proceedings of the 2018 International Symposium on Code Generation and Optimization*, 2018, pp. 113–125.
- [32] M. Y. Siraichi, V. F. d. Santos, C. Collange, and F. M. Q. Pereira, "Qubit allocation as a combination of subgraph isomorphism and token swapping," *Proceedings of the ACM on Programming Languages*, vol. 3, no. OOPSLA, pp. 1–29, 2019.
- [33] R. E. Tarjan and A. E. Trojanowski, "Finding a maximum independent set," *SIAM Journal on Computing*, vol. 6, no. 3, pp. 537–546, 1977.
- [34] D. Venturelli, M. Do, E. Rieffel, and J. Frank, "Temporal planning for compilation of quantum approximate optimization circuits," in *Scheduling and Planning Applications workshop (SPARK)*, 2017, p. 58.

- [35] K. Wei, E. Magesan, I. Lauer, S. Srinivasan, D. Bogorin, S. Carnevale, G. Keefe, Y. Kim, D. Klaus, W. Landers *et al.*, “Quantum crosstalk cancellation for fast entangling gates and improved multi-qubit performance,” *arXiv preprint arXiv:2106.00675*, 2021.
- [36] R. Wille, D. Große, L. Teuber, G. W. Dueck, and R. Drechsler, “RevLib: An online resource for reversible functions and reversible circuits,” in *Int’l Symp. on Multi-Valued Logic*, 2008, pp. 220–225, RevLib is available at <http://www.revlib.org>.
- [37] L. Xie, J. Zhai, Z. Zhang, J. Allcock, S. Zhang, and Y. Zheng, “Suppressing zz crosstalk of quantum computers through pulse and scheduling co-optimization,” *Proceedings of the 27th ACM International Conference on Architectural Support for Programming Languages and Operating Systems*, 2022.
- [38] F. Yan, S. Gustavsson, A. Kamal, J. Birenbaum, A. P. Sears, D. Hover, T. J. Gudmundsen, D. Rosenberg, G. Samach, S. Weber *et al.*, “The flux qubit revisited to enhance coherence and reproducibility,” *Nature communications*, vol. 7, no. 1, p. 12964, 2016.
- [39] D. Zajac, J. Stehlik, D. Underwood, T. Phung, J. Blair, S. Carnevale, D. Klaus, G. Keefe, A. Carniol, M. Kumph *et al.*, “Spectator errors in tunable coupling architectures,” *arXiv preprint arXiv:2108.11221*, 2021.
- [40] C. Zhang, A. B. Hayes, L. Qiu, Y. Jin, Y. Chen, and E. Z. Zhang, “Time-optimal qubit mapping,” in *Proceedings of the 26th ACM International Conference on Architectural Support for Programming Languages and Operating Systems*, 2021, pp. 360–374.
- [41] P. Zhao, D. Lan, P. Xu, G. Xue, M. Blank, X. Tan, H. Yu, and Y. Yu, “Suppression of static z z interaction in an all-transmon quantum processor,” *Physical Review Applied*, vol. 16, no. 2, p. 024037, 2021.
- [42] P. Zhao, K. Linghu, Z. Li, P. Xu, R. Wang, G. Xue, Y. Jin, and H. Yu, “Quantum crosstalk analysis for simultaneous gate operations on superconducting qubits,” *PRX quantum*, vol. 3, no. 2, p. 020301, 2022.
- [43] A. Zulehner, A. Paler, and R. Wille, “An efficient methodology for mapping quantum circuits to the ibm qx architectures,” *IEEE Transactions on Computer-Aided Design of Integrated Circuits and Systems*, vol. 38, no. 7, pp. 1226–1236, 2018.